Modal Analysis of Rotating Beam Structures Having Complex Configurations Employing Multi-Reference Frames

Jung Min Kim
Robot R&D Institute, Daewoo Shipbuilding & Marine Engineering Co., Ltd., Jeongwang-dong, Siheung-si, Kyonggi-do 429-793, Korea
Hong Hee Yoo*
School of Mechanical Engineering, Hanyang University, Seoul 133-791, Korea

A modeling method for the modal analysis of rotating beam structures having complex configurations employing multi-reference frames is presented in the present study. In most structural analysis methods, single reference frame is employed for the modal analysis. For simple structures such as single beam or single plate, the method of employing single reference frame usually provides rapidly converging accurate results. However, for general structures having complex configurations, such a method provides slowly converging, and often erroneous, results. In the present study, the effects of employing multi-reference frames on the convergence and the accuracy of the modal analysis of rotating beam structures having complex configurations are investigated.

Key Words : Reference Frame, Rotating Structure, Finite Element Method, Geometric Stiffening Effect, Dynamic Equilibrium, Velocity Transformation Matrix, Natural Frequency

1. Introduction

Designs of aircraft or spacecraft, which are undergoing large overall motion during their normal operation, necessitate dynamic modeling methods for structures undergoing large overall motion. Even though such design activities can be accomplished through experiments, it is often very difficult and expensive to realize the actual operation environment on Earth for the aircraft or the spacecraft. For instance, the gravitational field in space is much different from that on Earth. Also, fast rotational rigid body motion, that is one of normal operations of aircraft, is quite difficult to realize through an experiment. Therefore, designers naturally endeavor to simulate the operation by employing an analytical or a numerical method instead of employing an experimental method. The analytical (or numerical) method, however, needs to be accurate and efficient if the design task can be accomplished with satisfaction.

Several modeling methods have been developed for the analysis of structures undergoing large overall motion. Classical linear modeling method (Ho, 1977 ; Shabana and Wehage, 1982 ; Ahmed and Shabana, 1986) is widely used to predict dynamic characteristics of structures. This modeling method has several merits such as simplicity of formulation, ease of implementation in finite element methods, and available coordinate reduction techniques, which are often critically important for dynamic analysis of structures. However, classical modeling method often displays a critical flaw when the structure undergoes a large overall motion. Consequently, several nonlinear

* Corresponding Author,
E-mail : hhyoo@hanyang.ac.kr
TEL : +82-2-2220-0446; **FAX** : +82-2-2293-5070
School of Mechanical Engineering, Hanyang University, Seoul 133-791, Korea. (Manuscript **Received** May 2, 2005; **Revised** December 6, 2005)

modeling methods (Christensen and Lee, 1986) were introduced to resolve the problem of classical linear modeling method. However, these methods are inconvenient (so inefficient) for the modal analysis of structures undergoing overall motion. A three-step procedure (first finding dynamic equilibrium state, then linearizing the nonlinear equations at the equilibrium state, and finally performing modal analysis with the linearized equations) needs to be followed to obtain the modal characteristics. And, in contrast to the linear modeling method, these methods are not available the coordinate reduction technique. More recently, to avoid the inconvenience of nonlinear modeling methods, special linear modeling methods employing hybrid deformation variables (Kane et al., 1987; Yoo et al., 1995; Park and Yoo, 1997; Choi et al., 2005; Kim and Yoo, 2002; Lee et al., 2004) were introduced. However, only simple structures such as single beam or single plate are solved with the modeling methods in which single reference frame is employed.

In previous modeling methods, single reference frame (an inertial reference frame is usually employed in the nonlinear modeling methods and a local reference frame is employed in the special linear modeling methods) is employed. The method of employing single reference frame is simple and effective to analyze simple structures such as a beam or a plate. However, for general structures having complex configurations, such a method could provide slowly converging, and often erroneous, results.

In this paper, a modeling method employing multi-reference frames is proposed. The proposed modeling method employs finite element method to consider general structures having complex configuration. The modeling method employs lumped mass modeling technique that simplifies the derivation of equations of motion. The mass and the stiffness matrices can be easily obtained from the commercial finite element codes for static and dynamic analysis of structures. Elastic deformations are approximated with the modal matrix, which can be obtained from the mass and the stiffness matrices by solving the eigenvalue problem. Therefore, in contrast to the nonlinear modeling method, the proposed method is available the coordinate reduction techniques likewise the linear modeling method. The geometric stiffening effect that results from the centrifugal inertia force caused by large overall motion is also considered in the modeling method. To verify the rapid convergence and the accuracy of the proposed modeling method, some numerical examples are solved. The results obtained by the present modeling method employing multi-reference frames are compared to those of a modeling method of employing single reference frame.

2. Equations of Motion

2.1 Kinetic energy

Figure 1 shows the configuration of a structure i undergoing rigid body motion and elastic deformation. In the figure, i_0 denotes configuration of the structure undergoing only the rigid body motion. The structure i is discretized in the lumped mass model. This configuration is observed in the inertial reference frame X_1-X_2. $\bar{X}_1^i-\bar{X}_2^i$ is a body reference frame fixed on the structure, j represents a generic node of the discretized structure i and $\bar{x}_{j1}^i-\bar{x}_{j2}^i$ is a nodal reference frame fixed on the generic node j. In the figure, $\mathbf{R}^i$ is position vector of the origin of the $\bar{X}_1^i-\bar{X}_2^i$, θ^i is rotational coordinate of the $\bar{X}_1^i-\bar{X}_2^i$ measured in the X_1-X_2, $\bar{\mathbf{u}}_{rj}^i$ is a position

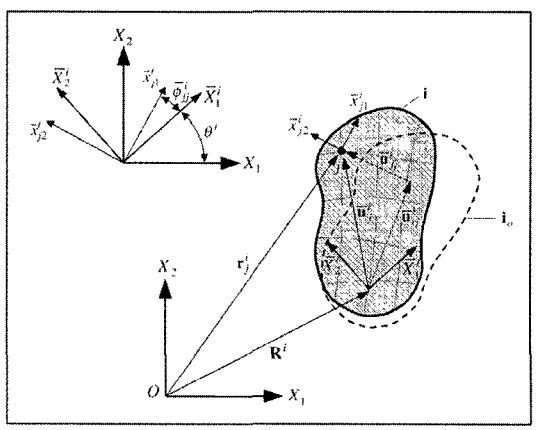

Fig. 1 Configuration of a structure undergoing rigid body motion and elastic deformation

vector of the j-th node in the undeformed state, $\bar{\mathbf{u}}_{fj}^i$ is pure translational elastic deformation and $\bar{\phi}_{fj}^i$ is pure rotational elastic deformation of the J-th node measured in the $\bar{X}_1^i-\bar{X}_2^i$. Using these quantities, position vector of the j-th node measured in the X_1-X_2 can be given as follows:

$$\mathbf{r}_j^i=\mathbf{R}^i+\mathbf{A}^i\bar{\mathbf{u}}_j^i=\mathbf{R}^i+\mathbf{A}^i(\bar{\mathbf{u}}_{rj}^i+\bar{\mathbf{u}}_{fj}^i) \tag{1}$$

where $\mathbf{A}^i$ is the orientation matrix of the $\bar{X}_1^i-\bar{X}_2^i$ with respect to the X_1-X_2. All nodal elastic deformations $\bar{\mathbf{u}}_f^i$ of the structure i can be approximated using the modal matrix.

$$\bar{\mathbf{u}}_f^i=\begin{bmatrix}\begin{Bmatrix}\bar{\mathbf{u}}_{f1}^i\\ \bar{\phi}_{f1}^i\end{Bmatrix}\\ \vdots\\ \begin{Bmatrix}\bar{\mathbf{u}}_{fNG^i}^i\\ \bar{\phi}_{fNG^i}^i\end{Bmatrix}\end{bmatrix}=\mathbf{N}^i\mathbf{q}_f^i=\begin{bmatrix}\begin{bmatrix}N_1^i\\ \mathbf{N}_{r1}^i\end{bmatrix}\\ \vdots\\ \begin{bmatrix}\mathbf{N}_{n^i{}_g^i}^i\\ \mathbf{N}_{rn^i}^i\end{bmatrix}\end{bmatrix}\mathbf{q}_f^i \tag{2}$$

where $\mathbf{N}^i$ is a reduced modal matrix which consists of mode vectors associated with several lower natural frequencies of the structure, $\mathbf{N}_j^i$ and $\mathbf{N}_{rj}^i$ are sub-matrices of $\mathbf{N}^i$ associated with the translational and rotational elastic deformation of the j-th node, n_g^i is the total number of nodes of the structure i and $\mathbf{q}_f^i$ is the modal coordinate. By using Eq. (2), the translational elastic deformation $\bar{\mathbf{u}}_{fj}^i$ of the j-th node can be represented as follows:

$$\bar{\mathbf{u}}_{fj}^i=\mathbf{N}_j^i\mathbf{q}_f^i \tag{3}$$

Velocity of the j-th node can be obtained by substituting Eq. (3) into Eq. (1) and differentiating the resulted equation with respect to time in the inertial reference frame. This yields

$$\dot{\mathbf{r}}_j^i=\dot{\mathbf{R}}^i+\mathbf{B}_j^i\dot{\theta}^i+\mathbf{A}^i\mathbf{N}_j^i\dot{\mathbf{q}}_f^i \tag{4}$$

where

$$\mathbf{B}_j^i\equiv\mathbf{A}_\theta^i\bar{\mathbf{u}}_j^i \tag{5}$$

Since $\bar{\mathbf{u}}_{rj}^i$ is a constant vector (a position vector of the j-th node in the undeformed state), in Eq. (4), the term related to the time derivative of $\bar{\mathbf{u}}_{rj}^i$ is disappeared. In Eq. (5), $\mathbf{A}_\theta^i$ is partial derivative of $\mathbf{A}^i$ with respect to θ^i. Let's define that m_j^i is the mass of the j-th node. Then the kinetic energy of the structure i can be described as follows:

$$T^i=\frac{1}{2}\begin{bmatrix}\dot{\mathbf{R}}\\ \dot{\theta}\\ \dot{\mathbf{q}}_f\end{bmatrix}^{iT}\begin{bmatrix}\mathbf{M}_{rr} & \mathbf{M}_{r\theta} & \mathbf{M}_{rf}\\ & \mathbf{M}_{\theta\theta} & \mathbf{M}_{\theta f}\\ \text{symmetric} & & \mathbf{M}_{ff}\end{bmatrix}^i\begin{bmatrix}\dot{\mathbf{R}}\\ \dot{\theta}\\ \dot{\mathbf{q}}_f\end{bmatrix}^i=\frac{1}{2}\dot{\mathbf{q}}^{iT}\mathbf{M}^i\dot{\mathbf{q}}^i \tag{6}$$

where, $\mathbf{M}^i$ and $\mathbf{q}^i$ are the mass matrix and the generalized coordinate vector for structure i. Symbols used in the above equation are defined as follows:

$$M_{rr}^i=\sum_{j=1}^{n_g^i}m_j^i\mathbf{I}\qquad \mathbf{M}_{r\theta}^i=\sum_{j=1}^{n_g^i}m_j^i\mathbf{B}_j^i\qquad \mathbf{M}_{rf}^i=\sum_{j=1}^{n_g^i}m_j^i\mathbf{A}^i\mathbf{N}_j^i$$
$$\mathbf{M}_{\theta\theta}^i=\sum_{j=1}^{n_g^i}m_j^i\mathbf{B}_j^{iT}\mathbf{B}_j^i\qquad \mathbf{M}_{\theta f}^i=\sum_{j=1}^{n_g^i}m_j^i\mathbf{B}_j^{iT}\mathbf{A}^i\mathbf{N}_j^i \tag{7}$$
$$\mathbf{M}_{ff}^i=\sum_{j=1}^{n_g^i}m_j^i\mathbf{N}_j^{iT}\mathbf{N}_j^i$$

$$\mathbf{q}^i=[\mathbf{R}^{iT}\ \theta^i\ \mathbf{q}_f^{iT}]^{iT} \tag{8}$$

2.2 Strain energy

Since the strain energy of the structures is only associated with elastic deformations of the structures, the strain energy of the structure i is can be described as follows:

$$U^i=\frac{1}{2}\bar{\mathbf{u}}_f^{iT}\bar{\mathbf{K}}^i\bar{\mathbf{u}}_f^i \tag{9}$$

where $\bar{\mathbf{K}}^i$ is the global stiffness matrix in the finite element method. By using Eq. (2) and Eq. (9), the strain energy can be written as follows:

$$U^i=\frac{1}{2}\begin{bmatrix}\mathbf{R}\\ \theta\\ \mathbf{q}_f\end{bmatrix}^{iT}\begin{bmatrix}0\ 0\ 0\\ 0\ 0\ 0\\ 0\ 0\ \mathbf{K}_{ff}\end{bmatrix}^i\begin{bmatrix}\mathbf{R}\\ \theta\\ \mathbf{q}_f\end{bmatrix}^i=\frac{1}{2}\mathbf{q}^{iT}\mathbf{K}^i\mathbf{q}^i \tag{10}$$

where, $\mathbf{K}_{ff}^i$ is the diagonal matrix defined as follows:

$$\mathbf{K}_{ff}^i=\mathbf{N}^{iT}\bar{\mathbf{K}}^i\mathbf{N}^i \tag{11}$$

2.3 Generalized force by geometric nonlinearity

To consider the geometric stiffening effect of a structure that consists of beam elements, work done by the axial force P during the lateral deflection should be considered. The geometric stiffening effect of an infinitesimal beam element due to lateral deflection is shown in Fig. 2. The axial length change of the infinitesimal beam element due to lateral deflection can be obtained as follows:

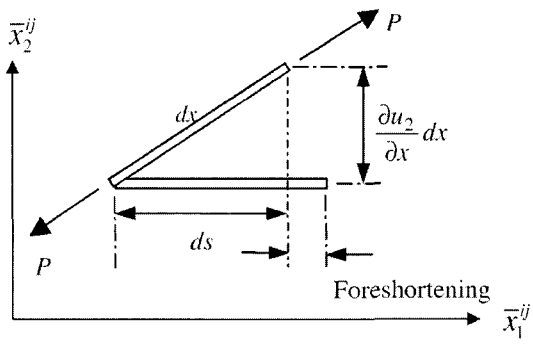

Fig. 2 Foreshortening of an infinitesimal beam element due to lateral deflection

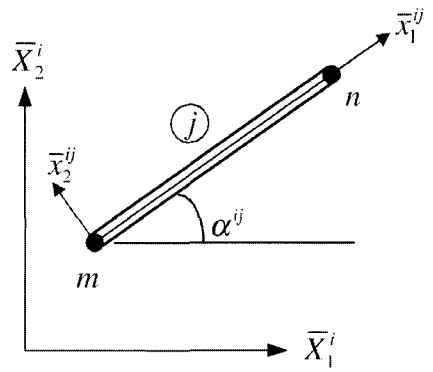

Fig. 3 Notations for i-th beam element

$$dx-ds=dx-\left[(dx)^2-\left(\frac{\partial u_2}{\partial x}\right)^2(dx)^2\right]^{1/2} \cong\frac{1}{2}\left(\frac{\partial u_2}{\partial x}\right)^2 dx \tag{12}$$

Since foreshortening occurs while the axial force acts on the element, the work done by the axial force is negative. Therefore, the work done by the axial force, which is invariant during the foreshortening, can be obtained as follows:

$$W_g^{ij}=-\frac{1}{2}\int_0^{l^{ij}} P^{ij}\left(\frac{\partial u_2^{ij}}{\partial x}\right)^2 dx \tag{13}$$

where l^{ij} is the length of the j-th beam element in the structure i; P^{ij} is the axial force acting on the beam element; u_2^{ij} is the lateral deflection of the beam element. Therefore, the virtual work done by the axial force of the structure i that is composed of n_e^i beam elements can be described as following equation.

$$\delta W_g^i=-\sum_{j=1}^{n_e^i}\int_0^{l^{ij}} P^{ij}\left(\frac{\partial u_2^{ij}}{\partial x}\right)\delta\left(\frac{\partial u_2^{ij}}{dx}\right) dx \tag{14}$$

By employing the shape function $\mathbf{S}^{ij}$ of a beam element, the axial and lateral deflection of beam element can be written as follows:

$$\begin{bmatrix} u_1^{ij} \\ u_2^{ij} \end{bmatrix}=\mathbf{S}^{ij}\mathbf{T}^{ij}\mathbf{q}_f^i \tag{15}$$

The shape function $\mathbf{S}^{ij}$ and $\mathbf{T}^{ij}$ in Eq. (15) can be given as follows:

$$\mathbf{S}^{ij}=\begin{bmatrix}\mathbf{S}_1^{ij} \\ \mathbf{S}_2^{ij}\end{bmatrix} =\begin{bmatrix} 1-\xi & 0 & 0 & \xi & 0 & 0 \\ 0 & 1-3\xi^2+2\xi^3 & l^{ij}(\xi-2\xi^2+\xi^3) & 0 & 3\xi^2-2\xi^2 & l^{ij}(\xi^3-\xi^2)\end{bmatrix} \tag{16}$$

where

$$\xi=\frac{x}{l^{ij}} \tag{17}$$

$$\mathbf{T}^{ij}\equiv\mathbf{C}^{ij}\mathbf{L}^{ij}\mathbf{N}^i \tag{18}$$

where

$$\mathbf{C}^{ij}=\begin{bmatrix} \cos\alpha^{ij} & \sin\alpha^{ij} & 0 & 0 & 0 & 0 \\ -\sin\alpha^{ij} & \cos\alpha^{ij} & 0 & 0 & 0 & 0 \\ 0 & 0 & 1 & 0 & 0 & 0 \\ 0 & 0 & 0 & \cos\alpha^{ij} & \sin\alpha^{ij} & 0 \\ 0 & 0 & 0 & -\sin\alpha^{ij} & \cos\alpha^{ij} & 0 \\ 0 & 0 & 0 & 0 & 0 & 1 \end{bmatrix} \tag{19}$$

$$\mathbf{L}^{ij}=\underbrace{\begin{bmatrix}\mathbf{0} & \mathbf{I}_{3\times3} & \mathbf{0} & \mathbf{0} & \mathbf{0} \\ \mathbf{0} & \mathbf{0} & \mathbf{0} & \mathbf{I}_{3\times3} & \mathbf{0}\end{bmatrix}}_{6\times3n_e^i} \tag{20}$$

($\mathbf{0}$: $6(m-1)$; $\mathbf{I}_{3\times3}$: $6(n-1)$; $\mathbf{0}$: $3n_e^i$)

In the above equations, $\mathbf{C}^{ij}$ and $\mathbf{L}^{ij}$ denote a transformation matrix and a Boolean matrix for beam element assembly, respectively. In Eq. (19), α^{ij} denotes the angle between the structure reference frame $\bar{X}_1^i-\bar{X}_2^i$ and the element reference frame $\bar{x}_1^{ij}-\bar{x}_2^{ij}$. In Eq. (20), m and n denote the node numbers of the j-th beam element, which are shown in Fig. 3.

Substituting Eq. (15) into Eq. (14), the virtual work created by the geometric stiffening effect can be obtained as follows:

$$\delta W_g^i=-\mathbf{q}_f^{iT}\mathbf{K}_g^{iT}\delta\mathbf{q}_f^i \tag{21}$$

In the above equation, $\mathbf{K}_g^i$ is the geometric stiffness matrix for structure i which can be defined as

$$\mathbf{K}_g^i \equiv \sum_{j=1}^{n_e^i} P^{ij}\mathbf{T}^{ij^T}\mathbf{G}^{ij}\mathbf{T}^{ij} \tag{22}$$

where

$$\mathbf{G}^{ij} \equiv \int_0^{l^{ij}} \mathbf{S}_{2,x}^{ij^T}\mathbf{S}_{2,x}^{ij}\,dx$$

$$= \frac{1}{l^{ij}}\begin{bmatrix} 0 & 0 & 0 & 0 & 0 & 0 \\ 0 & \frac{6}{5} & \frac{l^{ij}}{10} & 0 & -\frac{6}{5} & \frac{l^{ij}}{10} \\ 0 & \frac{l^{ij}}{10} & \frac{2(l^{ij})^2}{15} & 0 & -\frac{l^{ij}}{10} & -\frac{(l^{ij})^2}{30} \\ 0 & 0 & -\frac{l^{ij}}{10} & 0 & 0 & 0 \\ 0 & -\frac{6}{5} & -\frac{l^{ij}}{10} & 0 & \frac{6}{5} & -\frac{l^{ij}}{10} \\ 0 & \frac{l^{ij}}{10} & -\frac{(l^{ij})^2}{30} & 0 & -\frac{l^{ij}}{10} & \frac{2(l^{ij})^2}{15} \end{bmatrix} \tag{23}$$

where $\mathbf{S}_{2,x}^{ij}$ is the partial derivative of $\mathbf{S}_2^{ij}$ with respect to x. Using the Hooke's law, the axial force P^{ij} can be obtained as follows:

$$P^{ij} = E^{ij}a^{ij}\left(\frac{\partial u_1^{ij}}{\partial x}\right) = E^{ij}a^{ij}\mathbf{S}_{1,x}^{ij}\mathbf{q}_f^i \tag{24}$$

where E^{ij} is the Young's modulus of the beam element j in the structure i, a^{ij} is the cross sectional area of the element and

$$\mathbf{S}_{1,x}^{ij} = \frac{1}{l^{ij}}[-1\ 0\ 0\ 1\ 0\ 0] \tag{25}$$

From Eq. (21), the generalized force due to the geometric stiffening effect associated with $\mathbf{q}_f^i$ can be obtained as follows:

$$(\mathbf{Q}_g^i)_f = -\mathbf{K}_g^i\mathbf{q}_f^i \tag{26}$$

Finally, the generalized force can be expressed as follows:

$$\mathbf{Q}_g^i = \begin{Bmatrix} 0 \\ 0 \\ 0 \\ (\mathbf{Q}_g^i)_f \end{Bmatrix} \tag{27}$$

2.4 Equations of motion

By using the kinetic energy, the strain energy, and the generalized force by the geometric nonlinearity presented in the previous three sections, the equations of motion for structure that consists of nb substructures can be described as follows:

$$\mathbf{M}\ddot{\mathbf{q}} + \boldsymbol{\Phi}_\mathbf{q}^T\lambda = -\mathbf{K}\mathbf{q} + \mathbf{Q}_v + \mathbf{Q}_g \tag{28}$$

$$\boldsymbol{\Phi}(\mathbf{q}, t) = \mathbf{0} \tag{29}$$

In the above equation, $\mathbf{M}$ is the system mass matrix that is function of the rotational and modal coordinates, and $\mathbf{K}$ is the system stiffness matrix. They are defined as follows.

$$\mathbf{M} = diag(\mathbf{M}^1, \cdots, \mathbf{M}^{nb}) \tag{30}$$

$$\mathbf{K} = diag(\mathbf{K}_1, \cdots, \mathbf{K}^{nb}) \tag{31}$$

And $\mathbf{q}$ is the generalized coordinate of the system, $\boldsymbol{\Phi}$ is the constraints equation, $\boldsymbol{\Phi}_\mathbf{q}$ and λ are the constraint Jacobian matrix and the Lagrange multiplier vector that relates reaction force due to constraints, respectively. The notation $\mathbf{Q}_v$ is the generalized force due to centrifugal and Coriolis acceleration. It is given as follows.

$$\mathbf{Q}_v = [\mathbf{Q}_v^{1^T}, \cdots, \mathbf{Q}_v^{nb^T}]^T \tag{32}$$

where $\mathbf{Q}_v^i$ is

$$\mathbf{Q}_v^i = -\dot{\mathbf{M}}^i\dot{\mathbf{q}}^i + \frac{1}{2}\left[\frac{\partial}{\partial \mathbf{q}^i}(\dot{\mathbf{q}}^{i^T}\mathbf{M}^i\dot{\mathbf{q}}^i)\right]^T \tag{33}$$

And the generalized force of the system due to the geometric nonlinearity is

$$\mathbf{Q}_g = [\mathbf{Q}_g^{1^T}, \cdots, \mathbf{Q}_g^{nb^T}]^T \tag{34}$$

2.5 Equations for modal analysis

To perform modal analysis of rotating structures, the dynamic equilibrium position and the linearized equations of motion at the equilibrium need to be derived to obtain the mass and the stiffness matrices.

The equations of motion Eq. (28) employ independent and dependent coordinates. The independent coordinates become constant in the dynamic equilibrium position and the dependent coordinates vary with time. Therefore, the equations of motion must be expressed with the independent coordinates to obtain the dynamic equilibrium position. For the purpose, the recursive formulation is employed in this study.

First, the system coordinates can be partitioned as follows:

$$\mathbf{q} = [\mathbf{q}_d^T\ \mathbf{q}_i^T]^T \tag{35}$$

where $\mathbf{q}_d$ and $\mathbf{q}_i$ represent the dependent and independent coordinates, respectively.

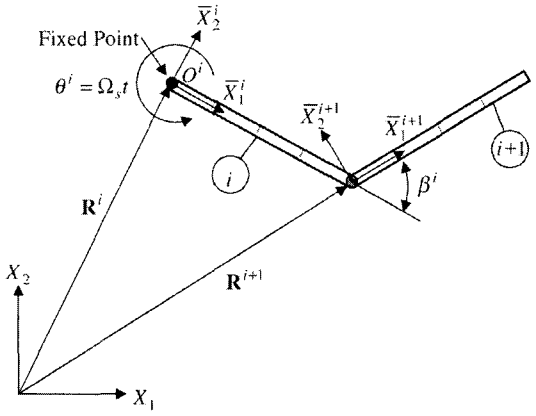

Fig. 4 Configuration of a two-beam structure

For clear explanation of the dependent and independent coordinates, consider the structure which is rigidly connected with two beam structures, the point O^i is fixed and the rotational speed (Ω_s) of the reference frame $\bar{X}_1^i-\bar{X}_2^i$ is constant as shown in Fig. 4.

For the structure, the dependent and independent coordinates are defined and related to the vectors in Eq. (8) as follows:

$$\mathbf{q}_d=\begin{bmatrix}\mathbf{R}^i\\ \theta^i\\ \mathbf{R}^{i+1}\\ \theta^{i+1}\end{bmatrix}=\begin{bmatrix}\text{Contant}\\ \omega t\\ \mathbf{R}^i+\mathbf{A}^i(\bar{\mathbf{u}}_{rj}^i+\mathbf{N}_j^i\mathbf{q}_f^i)\\ \theta^i+\mathbf{N}_{rj}^i\mathbf{q}_f^i+\beta^i\end{bmatrix} \tag{36}$$

$$\mathbf{q}_i=\begin{bmatrix}\mathbf{q}_f^i\\ \mathbf{q}_f^{i+1}\end{bmatrix} \tag{37}$$

Using the recursive formulation, the double differentiation of the system coordinates results in the following equation.

$$\ddot{\mathbf{q}}=\mathbf{B}_i\ddot{\mathbf{q}}_i+\gamma_i \tag{38}$$

in which $\mathbf{B}_i$ is the velocity transformation matrix which is mathematically defined as following equation and γ_i is the quadratic velocity vector of the independent coordinates.

$$\mathbf{B}_i=\begin{bmatrix}-\boldsymbol{\Phi}_{q_d}^{-1}\boldsymbol{\Phi}_{q_i}\\ \mathbf{I}\end{bmatrix} \tag{39}$$

Substituting Eq. (38) into Eq. (28) and pre-multiplying the equation by $\mathbf{B}_i^T$, one can obtain the following equation.

$$\mathbf{B}_i^T\mathbf{M}\mathbf{B}_i\ddot{\mathbf{q}}_i+\mathbf{B}_i^T(\mathbf{M}\gamma_i-\mathbf{Q})=\mathbf{0} \tag{40}$$

where

$$\mathbf{Q}=-\mathbf{K}\mathbf{q}+\mathbf{Q}_v+\mathbf{Q}_g \tag{41}$$

Note that the term containing the Lagrange multipliers are disappeared in Eq. (41), because of, the velocity transformation matrix $\mathbf{B}_i$ is the null space of the Jacobian matrix $\boldsymbol{\Phi}_q$.

In Eq. (40), one can obtain the dynamic equilibrium equation by letting $\dot{\mathbf{q}}_i=\ddot{\mathbf{q}}_i=\mathbf{0}$. Since the resulting dynamic equilibrium equation is generally nonlinear in terms of the independent coordinates, the dynamic equilibrium position can be obtained by using Newton-Raphson algorithm. Finally, the mass, damping and stiffness matrices can be obtained by linearizing Eq. (40) at the obtained dynamic equilibrium position. Thus, the mass, damping and stiffness matrices for the modal analysis can be obtained as follows:

$$\mathbf{M}^*=\mathbf{B}_i^T\mathbf{M}\mathbf{B}_i|_{q_2=q_i^*} \tag{42}$$

$$\mathbf{C}^*=\left[\frac{\partial}{\partial\dot{\mathbf{q}}_i}(\mathbf{B}_i^T\mathbf{M}\mathbf{B}_i\ddot{\mathbf{q}}_i+\mathbf{B}_i^T\mathbf{M}\gamma_i-\mathbf{B}_i^T\mathbf{Q})\right]_{q^2=q_i^*} \tag{43}$$

$$\mathbf{K}^*=\left[\frac{\partial}{\partial\mathbf{q}_i}(\mathbf{B}_i^T\mathbf{M}\mathbf{B}_i\ddot{\mathbf{q}}_i+\mathbf{B}_i^T\mathbf{M}\gamma_i-\mathbf{B}_i^T\mathbf{Q})\right]_{q^2=q_i^*} \tag{44}$$

where, $\mathbf{q}_i^*$ is the independent coordinates at the dynamic equilibrium position. To obtain the damping and stiffness matrix in Eq. (43) and Eq. (44) a well-known finite difference method is employed in the present study. Finally, the equation for the modal analysis can be obtained as follows:

$$\mathbf{M}^*\delta\ddot{\mathbf{q}}_i+\mathbf{C}^*\delta\dot{\mathbf{q}}_i+\mathbf{K}^*\delta\mathbf{q}_i=\mathbf{0} \tag{45}$$

3. Numerical Studies and Results

Figure 5 shows a rotating angled-beam structure. The angled-beam rotates in the plane with a constant angular speed Ω_s. The notation β shown in the figure denotes the angle between the horizontal beam and the skewed beam. $\bar{X}_1^1-\bar{X}_2^1$ is a reference frame which is fixed on the left end of horizontal beam. The mathematical model for the angled-beam structure can be derived by following the procedure presented in sec. 2.3 through

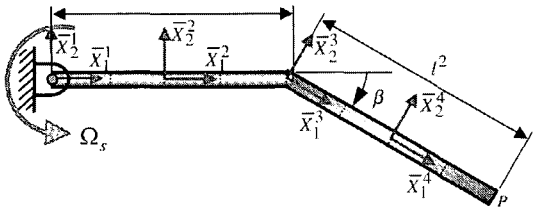

Fig. 5 Configuration of rotating angled-beam

Table 1 Properties of the angled-beam

E (N/m^2)	ρ (kg/m)	I (m^4)	A (m^2)	l^1 (m)	l^2 (m)
7×10^{10}	1.2	2×10^{-7}	4×10^{-4}	5	5

sec. 2.5 along with the finite element procedure. The geometric and the material properties of the beam are shown in Table 1. 32-beam elements are used for the numerical studies.

3.1 Dynamic equilibrium state

Before performing the modal analysis, the dynamic equilibrium positions of the free end P are computed employing single reference frame method and multi-reference frame method, when angle β is the right angle (90°). The results obtained by the two methods are shown in Figs. 6 and 7. The results obtained with a commercial code are also shown in the figure for the purpose of verification. Fully nonlinear beam elements are employed with the commercial code to obtain the dynamic equilibrium positions. The dynamic equilibrium positions are measured in the reference frame $\bar{X}_1^1-\bar{X}_2^1$. Figs. 6 and 7 show the dynamic equilibrium positions of the free end in $\bar{X}_1^1$ and $\bar{X}_2^1$ directions versus the angular speed. The figures show that the results employing multi-reference frames are in excellent agreement with those of the commercial code. However, the results obtained with the single reference frame become inaccurate as the angular speed increases. Since the modal analysis is performed using the equations of motion that are linearized at the dynamic equilibrium position, one can easily speculate that the modal analysis results obtained by employing the multi-reference frames should be more accurate than those obtained by employing the single reference frame.

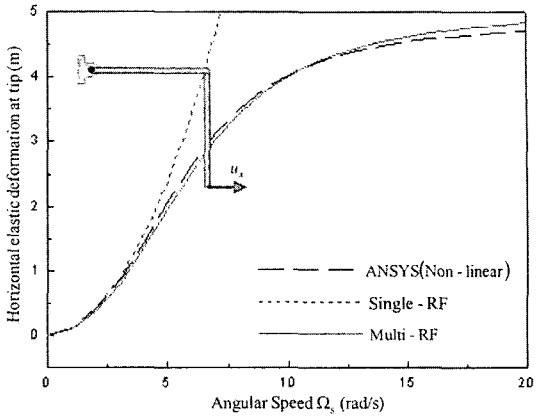

Fig. 6 Horizontal displacement at the free end ($\beta=90°$)

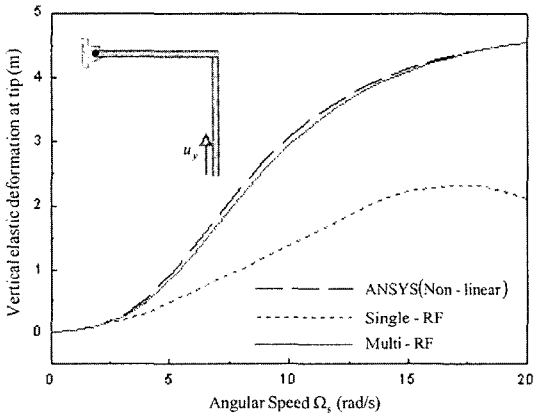

Fig. 7 Comparison of vertical displacement at free end ($\beta=90°$)

3.2 Natural frequencies

Figures 8-10 show the variation of the lowest three natural frequencies of the angled-beam structure versus the angular speed, when the angle β is 0°, 45°, 90°, respectively. These results are computed by employing single reference frame, multi-reference frames and the commercial code.

Since the fully nonlinear finite element formulation can be only employed to compute the dynamic equilibrium position, the linear finite element formulation should be employed for the modal analysis.

Figure 8 shows that the results employing single reference frame, multi-reference frames and the commercial code are in reasonable agreement. As shown in the figures, the natural frequencies

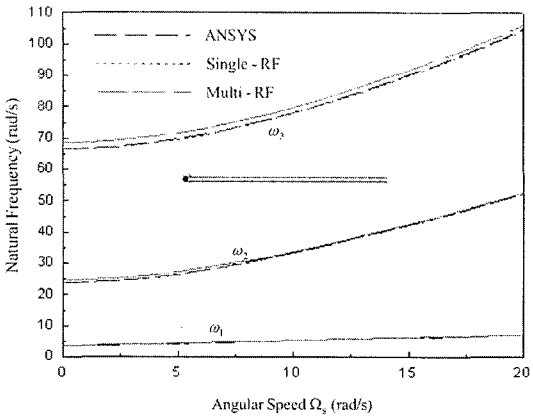

Fig. 8 Lowest three natural frequency variations versus angular velocity (β=0°)

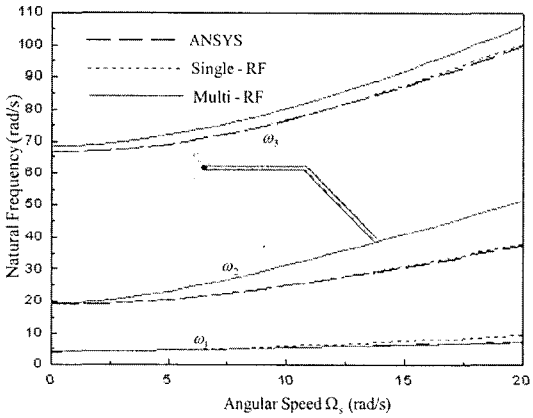

Fig. 9 Lowest three natural frequency variations versus angular velocity (β=45°)

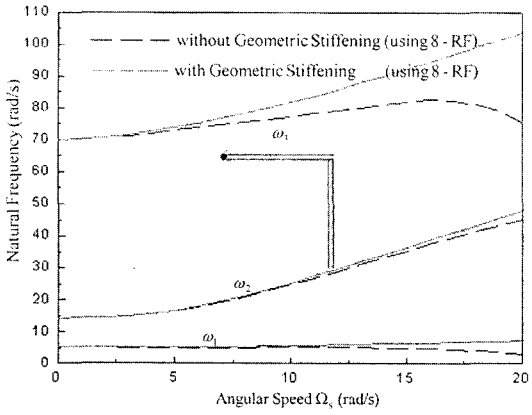

Fig. 10 Lowest three natural frequency variations versus angular velocity (β=90°)

increase as angular speed increases. This phenomenon is well known as the stiffening effect of the rotating structures. However, as shown in Figs. 9 and 10, as the angle and the angular speed increase, differences among the three results increase. In the previous section, it was shown that the dynamic equilibrium results employing multi-reference frames are the most accurate results among the three results.

Therefore, as the angle β of the structure and the angular speed increase, the natural frequencies employing multi-reference frames should be more accurate than those obtained by employing single reference frame and the commercial code.

Figure 11 shows the variation of the lowest three natural frequencies of the angled-beam structure versus the angular speed, when angle β is 90°. These results are obtained with and without the generalized force due to geometric non-linearity. In Fig. 12, 8-reference frames are used for the case in which the geometric stiffening effect is considered, and 16-reference frames are used for the case that does not consider the geometric stiffening effect. As shown in the figure, if the geometric stiffening effect is considered, the solution convergence can be obtained with less number of reference frames.

To investigate the convergence trends, when Ω_s=20 rad/s and β=90°, the lowest three natural frequencies versus the number of reference frames are tabulated in Table 2. 48-beam elements are

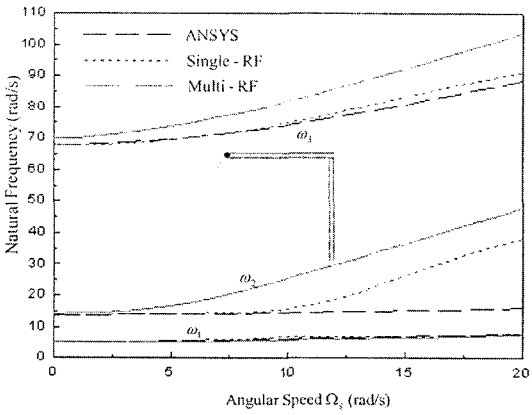

Fig. 11 Natural frequency variations with and without geometric stiffening (β=90°)

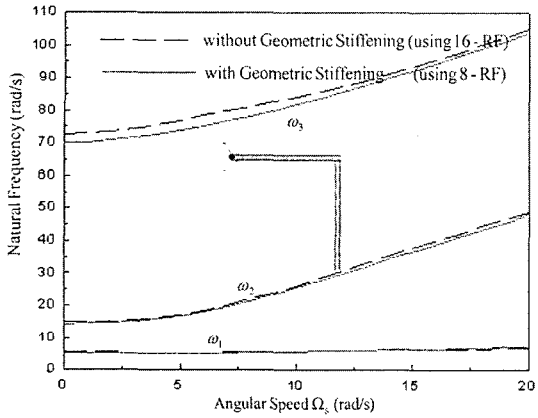

Fig. 12 Natural frequency variations with and without geometric stiffening (β=90°)

Table 2 Convergence of natural frequencies versus number of employed reference frames

RF	With geometric stiffening effect			Without geometric stiffening effect		
	ω_1	ω_2	ω_3	ω_1	ω_2	ω_3
2	6.40	34.61	63.77	Negative eigenvalue		
4	6.97	41.85	87.41			
6	7.11	46.46	96.21			
8	7.19	48.07	103.21	3.05	45.27	75.75
12	7.27	49.13	106.72	6.08	48.19	100.23
16	7.33	49.51	107.89	6.72	49.00	104.12

(Ω_s=20 rad/s and β=90°) (Units : rad/s)

used to obtain the results. In the cases which use 2, 4 and 6-reference frames, eigenvalues of the system become negative when the geometric stiffening effect is not considered. In other words, the mass or stiffness matrices of the system are not positive-definite. This is a critical disadvantage of the modeling method that does not consider the geometric stiffening effect. If the geometric stiffening effect is considered, one can obtain the converged natural frequencies with less number of reference frames.

4. Conclusions

In this study, a modeling method employing the multi-reference frames is proposed to find the modal characteristics of flexible structures. The modeling method can deal with the structures that have complex configuration and consider the geometric stiffening effect due to large overall motion. The effect of reference frames to the modal analysis accuracy is scrutinized through solving numerical examples. The numerical studies show that as the eccentricity of the structure and the angular speed increase, the results employing the multi-reference frames are more accurate than results employing the single reference frame. And if the geometric stiffening effect is considered in the modeling, it can obtain the modal analysis accuracy using smaller number of reference frames. It is also shown that the proposed modeling method provides more accurate natural frequencies than the commercial software.

Acknowledgments

This research was supported by Center of Innovative Design Optimization Technology (iDOT), Korea Science and Engineering Foundation.

References

Ahmed, A. and Shabana, A., 1986, "Dynamics of Inertia Variant Flexible Systems Using Experimentally Identified Parameters," *Journal of Mechanism, Transmissions, and Automation in Design*, Vol. 108, pp. 358~366.

Ahmed, A. and Shabana, A., 1988, *Dynamics of Multibody System*, John Wiley & Sons.

Christensen, E. and Lee, S., 1986, "Nonlinear Finite Element Modeling of the Dynamics of Unrestrained Flexible Structures," *Computer and Structures*, 23, pp. 819~829.

Dong Hwan Choi, Jung Hun Park, and Hong Hee Yoo, 2005, "Modal Analysis of Constrained Multibody Systems Undergoing Rotational Motion," *Journal of Sound and Vibration*, 280(1), pp. 63~76.

Eung-Min Park, Hong-Hee Yoo, 1997, "Dynamic Analysis of Multi-Beam Structures Considering Stiffening Effects Induced By Large Overall Rigid Body Motion," *Korean Society for Aeronautical and Space Science*, in Korea, Vol. 26, No. 2, pp. 40~46.

Ho, J., 1977, "Direct Path Method for Flexible

Multibody Spacecraft Dynamics," *Journal of Spacecraft and Rockets*, Vol. 14, pp. 102~110.

Kane, T., Ryan, R. and Banerjee, A., 1987, "Dynamics of Cantilever Beam Attached to a Moving Base," *Journal of Guidance, Control, and Dynamics*, 10, pp. 139~151.

Kim, S. K. and Yoo, H. H., 2002, "Vibration Analysis of Rotating Composite Cantilever Plates," *KSME International J.*, in Korea, 16(3), pp. 320~326.

Kim, S. K. and Yoo, H. H., 2002, "Vibration Analysis of Cantilever Plates Undergoing Translationally Accelerated Motion," *KSME International J.*, in Korea, 16(4), pp. 448~453.

Lee, S. H., Shin, S. H. and Yoo, H. H., 2004, "Flapwise Bending Vibration Analysis of Rotating Composite Cantilever Beams," *KSME International J.*, in Korea, 18(2), pp. 240~245.

Shabana, A. and Wehage, R. A., 1982, "Variable Degree of Freedom Component Mode Analysis of Inertia Variant Flexible Mechanical Systems," *Journal of Mechanical Design*, No. 82-DET-93, pp. 1~8.

Yoo, H., Ryan, R. and Scott, R., 1995, "Dynamics of Flexible Beams Undergoing Overall Motions," *Journal of Sound and Vibration*, 181(2), pp. 261~278.